Conjugate Heat Transfer in a Differentially Heated Porous Cavity Filled with Nanofluid

Muneer A. Ismael   &   Ahmed Abdulkareem Mahdi

Mechanical Engineering Department-Engineering College

University of Basrah-Basrah, Iraq.

Abstract: The conjugate natural convection-conduction heat transfer in a domain composed of nanofluids filled porous cavity heated by a vertical solid wall is studied under steady-state conditions. The vertical left wall of the solid is kept isothermal at hot temperature T_h. The vertical right wall of the solid is in contact with the nanofluid saturated porous medium contained in the cavity. The right vertical wall of the cavity is kept isothermally at the lower temperature T_c. The upper and lower horizontal walls are kept adiabatic. The governing equations of the heat transfer in the solid wall and heat and nanofluid flow, based on the Darcy model, in the nanofluid-saturated porous medium together with the derived relation of the interface temperature are solved numerically using the over-successive relaxation finite-difference method. A temperature independent nanofluids properties model is adopted. The investigated parameters are the nanoparticles volume fraction ϕ (0-0.2), Rayleigh number Ra (10-1000), solid wall to base-fluid saturated porous medium thermal conductivity ratio k_{wf} (0.1, 1, 10), and the solid wall thickness D (0.05-0.5). The results are presented in the conventional form; contours of streamlines and isotherms and the average Nusselt number. At a very low Rayleigh number $Ra=10$, an enhancement in heat transfer within the porous cavity with ϕ is observed. Otherwise, the heat transfer may be unchanged or deteriorated with ϕ depending on the wall thickness D and the conductivity ratio k_{wf}.

Keywords: Nanofluids, conjugate heat transfer, cavity, porous medium, Darcy model.

انتقال الحرارة المقترن خلال فجوة مسامية مشبعة بمائع نانوي و مسخنة تباينياً

منير عبد الجليل اسماعيل   &   أحمد عبد الكريم مهدي

جامعة البصرة ـ كلية الهندسة ـ قسم الهندسة الميكانيكية

الخلاصة

تم في هذا البحث دراسة انتقال الحرارة المقترن (حمل-توصيل) خلال حيز مكون من فجوة مسامية مشبعة بمائع نانوي و مسخنة بجــدار عمـــودي تحت ظرف الأستقرار. سطح الجدار العمودي الأيسر مثبت عند درجة حرارة ساخنة T_h و سطحه الأيمن في حالة تلامس مع المـــائع النـــانوي المشبع داخل الفجوة المسامية. جدار الفجوة الأيمن مثبت عند درجة حرارة باردة T_c . جدارا الفجوة الأعلى و الأسفل معزولان حرارياً. تم حل المعادلات الحاكمة لأنتقال الحرارة خلال الجدار الأيمن و معادلات انتقال الحرارة و جريان المائع النانوي (الذي بني على أساس نمــوذج دارسـي) خلال الفجوة وكذلك المعادلة المشتقة للسطح المشترك Interface بأستخدام طريقة الفروقات المحددة. خواص المائع النانوي اعتبرت ثابتة مــع درجة الحرارة. المتغيرات التي تمت دراستها هي النسبة الحجمية للجسيمات النانوية $\phi = (0-0.02)$ ، رقم رايلي $Ra=(10-1000)$ ، نسبة الموصلية الحرارية للجدار العمودي الى المائع الأساس $k_{wf}=(0.1, 1, 10)$ وسمك الجدار العمـــودي $D=(0.05-0.5)$. تم تمثيـــل النتـــائج بالطريقة المعروفة، أي خطوط دالة الجريان و التحارر و متوسط رقم نسلت. بينت النتائج بأنه عند قيمة $Ra=10$ هنالك تحسن في عملية انتقال الحرارة داخل الفجوة المسامية بزيادة النسبة الحجمية للجسيمات النانوية. فيما عدا ذلك، فأن انتقال الحرارة قد لا يتغيراو يتناقص مع ϕ اعتمادا على سمك الجدار D و نسبة الموصلية الحرارية k_{wf} .

Nomenclature				
D	dimensionless wall thickness	$Nu_{i,nf}$	local Nusselt number along the interface line
g	gravitational field (m s^{-2})	Ra	Rayleigh number $Ra = gK\rho_f \beta_f \left(Th - Tc\right)L / \left(\mu_f \alpha_f\right)$
k	thermal conductivity (W m^{-1} K^{-1})	T	temperature (K)
K	permeability of porous medium (m^2)	u	velocity component along x-direction (m s^{-1})
K_r	wall to nanofluid thermal conductivity ratio $K_r = k_w / k_{nf}$	v	velocity component along y-direction (m s^{-1})
k_{wf}	solid wall to base fluid thermal conductivity ratio $k_{wf} = k_w / k_f$	U	dimensionless velocity component along x-direction
L	square cavity wall length (m)	V	dimensionless velocity component along y-direction
Nu	average Nusselt number over the right cooled wall	x,y	Cartesian coordinates (m)
Nu_i	average Nusselt number over the interface line.	X,Y	dimensionless Cartesian coordinates
Greek symbols		*Subscripts*	
α	thermal diffusivity (m^2 s^{-1})	c	cold
β	thermal expansion coefficient (K^{-1})	f	fluid
ϕ	nanoparticles volume fraction	h	hot
μ	dynamic viscosity (Pa.s)	i	interface
θ	dimensionless temperature	nf	nanofluid
ρ	density (kg m^{-3})	p	solid nanoparticles
Ψ	dimensionless stream function	w	wall

1. Introduction

Natural convection inside enclosures has received a noticeable attention of investigation. This is due to their extensive applications in industry like cooling or heating systems, energy storage system (solar absorber), heat dissipation from electronic components, etc. Recently, the natural convection process is widely improved by using the technique of nanofluid. Nanofluid is a term refers to nanometer-sized metallic (or non-metallic) particles dispersed in a base fluid having, relatively, low thermal conductivity (in general) like water and ethylene glycol in order to obtain a fluid with improved thermophysical properties. The history of nanofluids investigation may refer to Choi and Eastman [1] where the term "nanofluids" was firstly introduced. Their theoretical study was as "hope" of heat transfer enhancement and actually their estimations concluded that dramatic reductions in heat exchanger pumping power could be obtained by dispersing copper nanoparticles in water. Pak and Cho [2] investigated experimentally the turbulent friction and heat transfer behavior of dispersed fluids (nanofluids term was not activated at that time). Their most relevant result was that the Nusselt number increased with increasing of volume concentration. However, they found that the convective heat transfer coefficient of the dispersed fluid at a certain volume fraction was 12% smaller than that of pure water. Therefore, they proposed that a better selection of nanaoparticles should be taken into account. Due to their extent applications and progressively developing published works concern with nanofluids, many researchers published review papers as in [3-5]. Khanafar et al. [6] studied the variances among different nanofluid models based on the physical properties of Cu-Water inside differentially heated rectangular enclosures. They reported that the variants among the models for nanofluid density have substantial effect on heat transfer rate at a given Grashof number. Wen and Ding [7] reported that the enhancement of convective heat transfer of nanofluids made of γ-Al_2O_3 and de-ionized water was particularly significant in the entrance region of a laminar flow region of copper tube. The same geometry of [6] was studied by khodadadi and Hosseinizadeh [8] but they directed the problem to be concerning with enhancing the thermal conductivity of phase change materials. Tiwari and Das [9] studied mixed convection inside two-sided lid-driven differentially heated square cavity. One of their conclusions was that nanoparticles were able to change the flow pattern of fluid from natural to forced convection regime. Choi et al. [10] reported that a volume fraction of 0.5% of AlN (Aluminum nitride) nanoparticles dispersed in transformer oil can increase the thermal conductivity by 8% and the overall heat transfer coefficient by 20%. Santra et al. [11] considered the problem of differentially heated square cavity by considering the nanofluid as a non-Newtonian fluid. Their novel result showed a considerable decrease in heat transfer for increase of solid volume fraction for any Rayleigh number. Abu-Nada et al. [12] considered various nanofluids inside horizontal concentric annuli. They showed that at intermediate value of Rayleigh number with low thermal conductive nanparticles, the Nusselt number decreased with solid volume fraction. Ho et al. [13] studied the natural convection of water-Al_2O_3 nanofluids filled three sizes of vertically square enclosures. The annuli of two differentially heated square ducts filled with TiO_2-Water nanofluid were investigated by Arefmanesh et al. [14]. Abu-Nada [15] and Abu-Nada and Chamkha [16] studied the effects of variable physical properties of nanofluids on natural convection.

Hence, it is worth it to mention here that all of the above surveyed works

dealt with viscous clear fluids (non-porous media) and that most of them reported that it was not always true that increasing the volume fraction of solid particles enhanced the heat transfer rate. It is found that a relatively a limited papers dealing with nanofluids saturated in porous media were published; and most of these papers studied the boundary layer flow. Nield and Kuzentov [17] examined the influence of nanoparticles natural convection past a vertical plate. Their analytical study was based on Brownian motion and thermophoresis (for nanofluids) and Darcy model (for porous media). Ahmed and Pop [18] studied numerically mixed convection boundary layer flow of the same problem of [30] using three different nanoparticles based on the conventional model of Tiwari and Das [9] which incorporates only the nanofluid volume fraction. They followed Darcy model also to interpret the flow in porous media. Gorla and Chamkha [19] considered natural convection boundary layer over a non-isothermal flat plate embedded in a porous medium. The natural convection boundary-layer flow about a sphere embedded in porous media was considered by Chamkha et al. [20]. More recently, Cimpean and Pop [21] studied fully developed steady-state mixed convection flow of nanofluids in a inclined porous channel. They used the Darcy model and Tiawri and Das model [9]. Hajipour and Dehkordi [22] considered mixed convection heat transfer of nanofluids based on the Brownian motion and thermophoresis in a vertical channel partially filled with highly porous medium using the Brinkman-Forchheimer model. Cheng [23] considered the studies of [19] and [20] but for a truncated cone. However, the field of nanofluids saturated in porous cavities is found published in very little works as in Sun and Pop [24] and recently, Chamkha and Ismael [25]. Sun and Pop [24] considered a triangular enclosure heated by a wall heater and filled with a porous medium and saturated with three different nanofluids. Their numerical study was based on the nanofluids model of [9] and the Darcy model for porous media. The heating wall of [25] was a triangular geometry in such a way that the inclined wall makes an inclined interface with the nanofluid saturated porous medium. Both studies [24] and [25] recorded in some circumstances the adverse relation between the Nusselt number and solid volume fraction i.e. decreasing of Nusselt number with the increase in the solid volume fraction.

Thus, what motivates us to continue in the field of natural convection in enclosures filled with nanofluids saturated porous media is the rareness of published works and hence, the incomplete views regarding this field of investigation. Moreover, the present authors are more interested in the conjugate conduction-convection heat transfer features and in particular in the case of Saeid [26]. Therefore, the present study considers steady conjugate conduction- convection inside a square cavity, filled with a nanofluid-saturated porous medium and heated by a vertical solid wall occupying one vertical wall of the square cavity.

2. Mathematical modeling

Figure 1 is a schematic illustration of the problem under consideration. It is a two-dimensional square domain with length L, the left side is a solid wall like a block with thickness d, kept isothermally at higher temperature T_h. The thickness d is varied while the overall domain is kept as a square. The inner surface of the solid wall is in contact with the contents-saturated porous medium forming the remainder domain. The upper and lower walls of the overall domain are kept adiabatic. The right vertical wall is cooled at constant temperature T_c. All of the boundaries are assumed impermeable. The pores between the solid matrix are assumed to be uniform and undeformable. The fluid filling the pores is composed of a base fluid (water) and nanoparticles forming a nanofluid.

They (the base fluid and the nanoparticles) are assumed to be in thermal equilibrium and no slip occurs between them. The nanofluid is assumed incompressible. Also, a thermal equilibrium between the nanofluid and the solid matrix is assumed to exist. The convective (slow) motion of the nanofluid in the saturated porous medium is considered to satisfy the Darcy model and the Boussinesq approximation $\rho=\rho_o(1-\beta(T-T_o))$. The governing equations based on these assumptions together with adopting Tiwari and Das [9] nanofluid model can be written as:

Continuity:

$$\frac{\partial u}{\partial x}+\frac{\partial v}{\partial y}=0 \qquad (1)$$

Momentum (x- direction)

$$u=-\frac{K}{\mu_{nf}}\left(\frac{\partial p}{\partial x}\right) \qquad (2)$$

Momentum (y- direction)

$$v=-\frac{K}{\mu_{nf}}\left(\frac{\partial p}{\partial y}+\rho_{nf}g\right) \qquad (3)$$

The usual way of eliminating the pressure terms from momentum equations is by differentiating Eq. (2) with respect to y and Eq. (3) with respect to x and then subtracting the results. So the final dimensional form of the momentum equation is:

$$\frac{\partial u}{\partial y}-\frac{\partial v}{\partial x}=-\frac{gK\left(\phi\rho_p\beta_p+(1-\phi)\rho_f\beta_f\right)}{\mu_{nf}}\frac{\partial T_{nf}}{\partial x} \qquad (4)$$

Energy (for nanofluid)

$$u\frac{\partial T_{nf}}{\partial x}+v\frac{\partial T_{nf}}{\partial y}=\alpha_{nf}\left(\frac{\partial^2 T_{nf}}{\partial x^2}+\frac{\partial^2 T_{nf}}{\partial y^2}\right) \qquad (5)$$

Energy (for the solid wall)

$$\frac{\partial^2 T_w}{\partial x^2}+\frac{\partial^2 T_w}{\partial y^2}=0 \qquad (6)$$

where β is the thermal expansion coefficient, ρ is the density, K is the permeability of the porous medium, μ is the dynamic viscosity, α is thermal diffusivity of the porous medium and ϕ is nanoparticles volume fraction. The subscripts p, f, nf, and w stand for solid nanoparticles, base fluid, nanofluid, and rectangular wall, respectively. Numerous formulations for the thermo-physical properties of nanofluids are proposed in the literature. In the present study, we are adopting the relations which depend on the nanoparticles volume fraction only and which were proven and used in many previous studies as follows:

Thermal diffusivity (Abu-Nada [15]):

$$\alpha_{nf}=\frac{k_{nf}}{\left(\rho C_p\right)_{nf}} \qquad (7)$$

Heat capacity (Khanafer et al. [6]):

$$\left(\rho Cp\right)_{nf}=(1-\phi)\left(\rho Cp\right)_f+\phi\left(\rho Cp\right)_p \qquad (8)$$

Thermal conductivity, based on Maxwell-Garnetts

$$k_{nf}=\frac{\left(k_p+2k_f\right)-2\phi\left(k_f-k_p\right)}{\left(k_p+2k_f\right)+\phi\left(k_f-k_p\right)}k_f \qquad (9)$$

Viscosity (Brinkman [27])

$$\mu_{nf}=\frac{\mu_f}{(1-\phi)^{2.5}} \qquad (10)$$

where k and (ρC_p) represent the thermal conductivity and heat capacity, respectively.

Introducing the following dimensionless set: $D=d/L$ $X=x/L$, $Y=y/L$, $U=uL/\alpha_f$, $V=vL/\alpha_f$, $\theta_{nf}=(T_{nf}-T_c)/(T_h-T_c)$, $\theta_w=(T_w-T_c)/(T_h-T_c)$, and the dimensionless definition of the stream function as: $U=\partial\Psi/\partial Y$, $V=-\partial\Psi/\partial X$, the set of Equations (4), (5), and (6) can be rewritten for the nanofluid-saturated porous medium as

$$\frac{1}{(1-\phi)^{2.5}} \nabla^2 \Psi = -Ra\left[(1-\phi)+\phi\left(\rho_p/\rho_f\right)\left(\beta_p/\beta_f\right)\right]\frac{\partial\theta_{nf}}{\partial X}$$

(11)

$$\frac{\partial\Psi}{\partial Y}\frac{\partial\theta_{nf}}{\partial X}-\frac{\partial\Psi}{\partial X}\frac{\partial\theta_{nf}}{\partial Y}=\frac{\alpha_{nf}}{\alpha_f}\nabla^2\theta_{nf}$$

(12)

and for the solid wall

$$\nabla^2\theta_w = 0$$

(13)

where $\nabla^2 = \partial^2/\partial x^2 + \partial^2/\partial y^2$ is the Laplace operator and Ra is the Rayleigh number of the porous media defined as $Ra = gK\rho_f\beta_f\left(Th-Tc\right)L/\left(\mu_f\alpha_f\right)$.

Equations (11) to (13) are subjected to the following boundary conditions:

Ψ=0 on the solid boundaries.

θ_{nf}=0 on the right vertical wall, X=1, $0\leq Y\leq 1$

$\partial\theta_{nf,w}/\partial Y$=0 on the upper horizontal wall $0< X <1$, Y=1 and on the horizontal lower wall $0< X <1$, Y=0.

θ_w=1 on the vertical right wall, X=0, $0 \leq Y \leq 1$.

At the interface between the solid wall and the fluid-saturated porous medium, the equilibrium state is assumed to be verified. Therefore, both the temperatures and the heat fluxes are the same;

$\theta_{nf}= \theta_w$ and $k_w\dfrac{\partial\theta_w}{\partial x} = k_{nf}\dfrac{\partial\theta_{nf}}{\partial x}$ or:

$$\frac{\partial\theta_{nf}}{\partial x} = K_r\frac{\partial\theta_w}{\partial x}$$

(14)

where K_r is the thermal conductivity ratio,

$$K_r = \frac{k_w}{k_{nf}} = \frac{\left(k_p+2k_f\right)+\phi\left(k_f-k_p\right)}{\left(k_p+2k_f\right)-2\phi\left(k_f-k_p\right)}\frac{k_w}{k_f}$$

(15)

It is worth to mention here that when ϕ =0,

the value of K_r becomes: $k_{wf}= k_w/k_f$, which shows the effect of wall thermal conductivity k_w on the heat transfer within the porous cavity.

The local Nusselt number along the interface within the nanofluid-saturated porous medium side can be written as:

$$Nu_{i,nf} = -\frac{k_{nf}}{k_f}\left.\frac{\partial\theta_{nf}}{\partial X}\right)_i$$

(16)

The average Nusselt numbers of interest are calculated on the interface (for the porous medium) and on the vertical right wall, respectively as:

$$Nu_i = \int_0^1 Nu_{i,nf}\,dY$$

(17)

$$Nu = -\frac{k_{nf}}{k_f}\int_0^1 \left.\frac{\partial\theta_{nf}}{\partial X}\right)_{X=1} dY$$

(18)

Due to energy balance, the overall heat transfer entering to the porous cavity from the interface line must be equal to that leaving the cavity from the right wall. Hence, the following energy balance can be employed for checking the accuracy of the numerical solution:

$$Nu_i = Nu$$

(19)

3. Numerical solution and validations

The final form of the governing equations set (Eqs. (11), (12) and (13)) are discretized uniformly ($\Delta X=\Delta Y$) over the square domain using the central finite-difference method. The values of the dimensionless solid wall D are varied with care in such a way that the interface must be localized on grid nodes. The boundary condition Eq.(14) is interpreted numerically by taking three points backward temperature gradient for the

solid wall and three points forward temperature gradient through the porous medium and since $\theta_{nf} = \theta_w$, hence, the following difference equation is invoked to compute the interface temperature:

$$\theta_i(i,j) = \frac{4\theta_{nf}(i+1,j) - \theta_{nf}(i+2,j) + K_r[4\theta_w(i-1,j) - \theta_w(i-2,j)]}{3(1+K_r)}$$

(20)

The descretized equations of the other situations are stated in Appendix A. Gauss-Seidel iteration procedure with Over Successive Relaxation (OSR) method is followed in the solution. The iteration is terminated when the following criterion is satisfied;

$$max\left[\left[\frac{\chi_{new}(i,j) - \chi_{old}(i,j)}{\chi_{old}(i,j)}\right]\right] \leq 10^{-6}$$

(21)

χ denotes any variable, Ψ, θ_{nf} or θ_w. Now, the choice of grid size requires some effort. The suitable grid size was based not only on the steadiness of say Nusselt number, but also on the verification of energy balance through the domain i.e. Equation (19). It is found that these conditions are sensitive to the value of the Rayleigh number. Figure 2 presents grid dependency behavior for $Ra=1000$, $D=0.1$, $k_{wf}=1$, with volume fraction $\phi=0.1$. Accordingly, a grid size of 71x71 was chosen in the numerical solution as a compromise between the accuracy and the running time.

The numerical methodology was coded in Matlab. The steps of numerical calculations are presented in Appendix B. To check the validity of the present code, a comparison with selective data from the published literature was carried out. However, the comparison was made with two different cases namely: conjugate horizontally heating (Saied [26]) and resolving, using the present code, conjugate Darcy-Bénard convection (Saleh et al. [28]). Figure 3 shows a selective comparative case with [26], while Table 1 presents some comparative data with both

[26] and [28]. It is obvious that good agreement is obtained, knowing that different numerical techniques were followed in these two different works. As a result, the confidence in the present numerical solution is enhanced.

4. Results and Discussion

The numerical results represented by the isotherms, streamlines, and average Nusselt number are presented in this section. The studied parameters ranges are: Rayleigh number $Ra=10$-1000, wall thickness $D=0.05$-0.5, solid volume fraction $\phi=0.0$-20%, and the thermal conductivity of wall to fluid (water) ratio $k_{wf}=0.1, 1, 10$. The considered nanoparticle is copper (Cu) which has thermophysical properties presented in Table 2.

Figure 4 shows the effect of Ra on the isotherms and streamlines for $D=0.3$, $\phi=0.1$ and $k_{wf}=1.0$. At very low Rayleigh number ($Ra=10$), the isotherms of the porous domain seem to be vertical, and since the heating is horizontal (differentially heated) so that, this implies to that the heat is transferred by conduction. Increasing Rayleigh number ($Ra=500$-1000), the isotherms within the porous domain become mostly horizontal which implies to convection dominance. This result is well known in the literature. On the right of Fig. 4, the strength of streamlines increases noticeably with Ra. The mechanism of forming such streamline is as follow: the fluid closest to the left hot wall (interface) is heated, and then it moves to the right cold wall (due to differentially heating) and moves up due to convection (Buoyancy force). When it becomes closer to the upper adiabatic wall, it turns to the right and falls down to the lower adiabatic wall. Hence, a single vortex of clockwise rotation (negative sign) is formed within the porous domain.

Figure 5 presents the effect of wall thermal conductivity on the isotherms and

streamlines for D=0.3, ϕ=0.1, and Ra=1000. Since we considered only one fluid type (water) hence the ratio k_{wf} reflects the effect of wall thermal conductivity. At very low wall conductivity (k_{wf}=0.1) the wall thermal resistance is very high accordingly, hence a steeper gradient of isotherms within the wall is seen and less amount of heat is transferred to the porous domain. Increase of k_{wf}, lead to reduce the wall thermal resistance. This can be characterized by the reduction of isotherms gradient within the wall and the convection activation within the porous cavity. The streamline shown in the right of Fig. 5 also emphasizes the effect of wall thermal conductivity; where the streamlines are strengthen with increasing k_{wf}. On the other hand, the effect of wall thickness D is presented in Fig. 6. In contrast with Fig. 5, the wall thermal resistance is directly proportional with D, so that and as shown in Fig. 6, when D is increased from 0.05 to 0.5, the temperature (isotherm) gradient within the wall is increased with less convection amount within the porous domain. However, Figs. 5 and 6 indicate to the fact that the thermal resistance of the wall is inversely proportional with its thermal conductivity and directly with its thickness.

The effect of solid volume fraction ϕ on the behavior of isotherm and streamlines is presented for two Rayleigh numbers Ra=10 and Ra=1000 in Figs. 7 and 8 respectively. No evident influence of ϕ can be drawn from these two figures except that at Ra=1000, the streamlines closer to the vertical walls are thinner for lower ϕ values. To understand the effect of ϕ, the average Nusselt number is plotted against ϕ, Ra, and D as presented in Figs. 9-12. In Fig. 9, the wall thickness D and conductivity ratio k_{wf} are fixed while the other two parameters are varied. It is clear that the average Nusselt number Nu is increased with ϕ at very low Rayleigh (Ra=10), otherwise, Nu is slightly

deteriorated as in Ra= 500 and 1000. Fig. 10 also enhance this behavior where it is seen that increasing the solid volume fraction ϕ enhance Nu only when $Ra <$ 100. The reason of such behavior refers to that adding solid nanoparticles increase not only the thermal conductivity of the nanofluid (Eq. (9)), but the viscosity (Eq. (10)) and density [16] are increased also which in turn increases the effect of viscous and inertia forces. At very low Ra, the viscous and inertia are already small so that their effect remains small despite increasing ϕ i.e. the effect of the enhanced thermal conductivity will overcome the effect of these two forces. But at higher values of Ra, where the viscous and inertia are significant, the increase of ϕ will enhance these two forces over the thermal conductivity, so a deterioration of Nu is recorded. This behavior was reported in many published works as in [10, 15-16, 24-25]. The effect of wall thickness on Nu is depicted in Fig. 11. In general, increasing D decreases Nu because of the increased thermal resistance of the wall which resists the heat transferred to the porous cavity. No significant effect of ϕ on Nu at high D values ($D \geq$0.2) is recorded from this figure. At lowest D (0.05), about 12% reduction in Nu is seen when ϕ increased from 0 to 20%. The effect of wall to fluid thermal conductivity ratio k_{wf} on Nu is plotted in Fig. 12. No significant effect of ϕ on Nu at low k_{wf} values ($k_{wf} \leq$1) is recorded while at high k_{wf}, about 12% reduction in Nu when ϕ increased from 0 to 20% is seen. However the reduction of Nu recorded in Figs. 11-12 occurs at the largest values of Nu where in this case the viscous and inertia forces are significant. Figures 13 and 14 depict the effect of Ra on Nu for different values of D and k_{wf}. As it expected, increasing of Ra leads to enhance the convection and hence increasing Nu. But this relation is very limited when the wall resistance posses high value as in D=0.5 (Fig. 13) and in k_{wf}=0.1 (Fig. 14). Eventually, the local

Nusselt number along the interface within the nanofluid-saturated porous medium $Nu_{i,nf}$ is depicted in Fig. 15 for D=0.2 and k_{wf}=1 and different Ra and ϕ values.

5. Conclusions

The problem of steady conjugate natural convection-conduction heat transfer in a square porous cavity heated differentially and filled with nanofluids was investigated numerically using Over Successive Relaxation (OSR) finite-difference method. The following remarks are concluded from the numerical results:

1- The heat transfer within nanofluids-saturated porous media may be enhanced or deteriorated with increasing the nanoparticles volume fraction. This significantly depends on the Rayleigh number and the solid wall thickness, where when $Ra \leq 100$, the average Nusselt number is an increasing function of volume fraction regardless of the other parameters, when $Ra > 100$, an influence of the solid wall thickness on the Nusselt number is originated.

2- The natural convection inside the nanofluid-saturated porous medium cavity is enhanced with increasing the solid wall conductivity and decreasing its thickness, and vice versa.

3- The most common effect of the Rayleigh number on the Nusselt number is held in this study, i.e. the Nusselt number is an increasing function of the Rayleigh number.

References

[1] S.U.S. Choi, J.A. Eastman, Enhancing thermal conductivity of fluids with nanoparticles, ASME International Mechanical Engineering Congress & Exposition San Francisco, CA; 1995.

[2] B.Ch. Pak, Y.I. Cho, Hydrodynamic and heat transfer study of dispersed fluids with submicron metallic oxide particles, Exp. Heat Transfer 11 (1998) 151-170

[3] X.Q. Wang, A.S. Mujumdar , Heat transfer characteristics of nanofluids: a review, Int. J. Thermal Sci. 46 (2007) 1–19

[4] D. Wen, G. Lin, S Vafaei, K. Zhang, Review of nanofluids for heat transfer applications, Particuology 7 (2009) 141–150

[5] S. Kakaç, A. Pramuanjaroenkij, Review of convective heat transfer enhancement with nanofluids, Int. J. Heat Mass Transfer 52 (2009) 3187–3196.

[6] K. Khanafer, K. Vafai, M. Lightstone, Buoyancy-driven heat transfer enhancement in a two-dimensional enclosure utilizing nanofluids, Int. J. Heat Mass Transfer 46 (2003) 3639–3653.

[7] D. Wen, Y. Ding, Experimental investigation into convective heat transfer of nanofluids at the entrance region under laminar flow conditions, Int. J. Heat Mass Transfer 47 (2004) 5181–5188

[8] J.M. Khodadadi, S.F. Hosseinizadeh, Nanoparticle-enhanced phase change materials (NEPCM) with great potential for improved thermal energy storage, Int. Commun. Heat Mass Transfer 34 (2007) 534–543.

[9] R.K. Tiwari, M.K. Das, Heat transfer augmentation in a two-sided lid-driven differentially heated square cavity utilizing nanofluids, Int. J. Heat Mass Transfer 50 (2007) 2002–2018

[10] C. Choi, H.S. Yoo, J.M. Oh, Preparation and heat transfer properties of nanoparticle-in-transformer oil dispersions as advanced energy-efficient coolants, Curr. Appl. Phys. 8 (2008) 710–712.

[11] A.K. Santra, S. Sen, N. Chakraborty, Study of heat transfer augmentation in a differentially heated square cavity using copper–water nanofluid, Int. J. Thermal Sci. 47 (2008) 1113–1122.

[12] E. Abu-Nada, Z. Masoud, A. Hijazi, Natural convection heat transfer enhancement in horizontal concentric annuli using nanofluids, Int. Commun. Heat Mass Transfer 35 (2008) 657–665

[13] C.J. Ho, W.K. Liu, Y.S .Chang, C.C. Lin, Natural convection heat transfer of alumina-water nanofluid in vertical square enclosures: An experimental study, Int. J. Thermal Sci. 49 (2010) 1345-1353.

[14] A. Arefmanesh, M. Amini, M. Mahmoodia, M. Najafi, Buoyancy-driven heat transfer analysis in two-square duct annuli filled with a nanofluid, Eur. J. Mech. B/Fluids 33 (2012) 95–104.

[15] E. Abu-Nada, Effects of variable viscosity and thermal conductivity of Al_2O_3–water nanofluid on heat transfer enhancement in natural convection, Int. J. Heat Fluid Flow 30 (2009) 679–690

[16] E. Abu-Nada, Ali J. Chamkha, Effect of nanofluid variable properties on natural convection in enclosures filled with a CuO-EG-Water nanofluid, Int. J. Thermal Sci. 49 (2010) 2339-2352.

[17] D.A. Nield, A.V. Kuznetsov, The Cheng–Minkowycz problem for natural convective boundary-layer flow in a porous medium saturated by a nanofluid, Int. J. Heat Mass Transfer 52 (2009) 5792–5795

[18] S. Ahmad, I. Pop, Mixed convection boundary layer flow from a vertical flat plate embedded in a porous medium filled with nanofluids, Int. Commun. Heat Mass Transfer 37 (2010) 987–991

[19] R.S.R. Gorla, A. Chamkha, Natural convective boundary layer flow over a non isothermal vertical plate embedded in a porous medium saturated with a nanofluid, Nanosc. Microsc. Therm. 15 (2011) 81–94.

[20] A. Chamkha, R.S.R. Gorla, K. Ghodeswar, Non-similar solution for natural convective boundary layer flow over a sphere embedded in a porous medium saturated with a nanofluid, Transp. Porous Med. 86 (2011) 13–22.

[21] D.S. Cimpean, I. Pop, Fully developed mixed convection flow of a nanofluid through an inclined channel filled with a porous medium, Int. J. Heat Mass Transfer 55 (2012) 907–914

[22] M. Hajipour, A.M. Dehkordi, Analysis of nanofluid heat transfer in parallel-plate vertical channels partially filled with porous medium, Int. J. Thermal Sci. 55 (2012) 103–113

[23] C-Y Cheng, Natural convection boundary layer flow over a truncated cone in a porous medium saturated by a nanofluid, Int. Commun. Heat Mass Transfer 39 (2012) 231–235.

[24] Q. Sun, I. Pop, Free convection in a triangle cavity filled with a porous medium saturated with nanofluids with flush mounted heater on the wall, Int. J. Thermal Sci. 50 (2011) 2141–2153

[25] A.J. Chamkha, M.A. Ismael, Conjugate heat transfer in a porous cavity filled with nanofluids and heated by a triangular thick wall, Int. J. Therm. Sci. 67 (2013) 135–151

[26] N.H. Saeid, Conjugate natural convection in a porous enclosure: effect of conduction in one of the vertical walls, Int. J. Thermal Sci. 46 (2007) 531–539.

[27] H.C. Brinkman, The viscosity of concentrated suspensions and solutions, J. Chem. Phys. 20 (1952) 571.

[28] H. Saleh, N.H. Saeid, I. Hashim, Z. Mustafa, Effect of Conduction in Bottom Wall on Darcy–Bénard Convection in a Porous Enclosure, Transp Porous Med 88 (2011) 357–368

Table 1. Comparison of the average Nusselt numbers with other works – conjugate cases, pure fluid ($\phi = 0$)

Ra	D	k_{wf}	Saeid [26]	Saleh et al. [28]	Present
			Nu	Nu	Nu
500	0.1	0.44	2.333	-	2.334
1000	0.4	2.4	3.511	-	3.49
1000	0.2	0.1	-	0.446	0.484
1000	0.5	1	-	1.566	1.589

Table 2. Thermo physical properties of base fluid and Cu nanoparticles [12]

Physical property	base fluid (water)	Cu
C_p (J/kg/K)	4179	385
ρ(kg/m^3)	997.1	8933
k (W/m/K)	0.613	401
β x 10^{-5} (1/K)	21	1.67
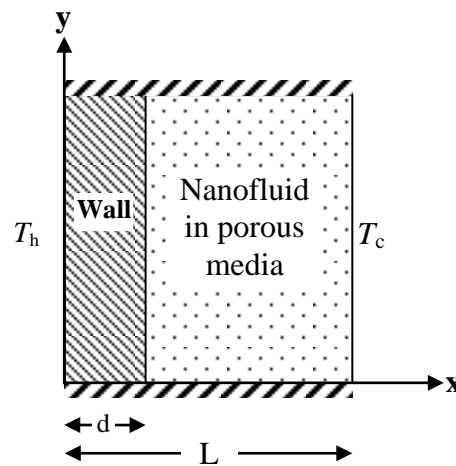
Fig.1 Schematic illustration of the problem
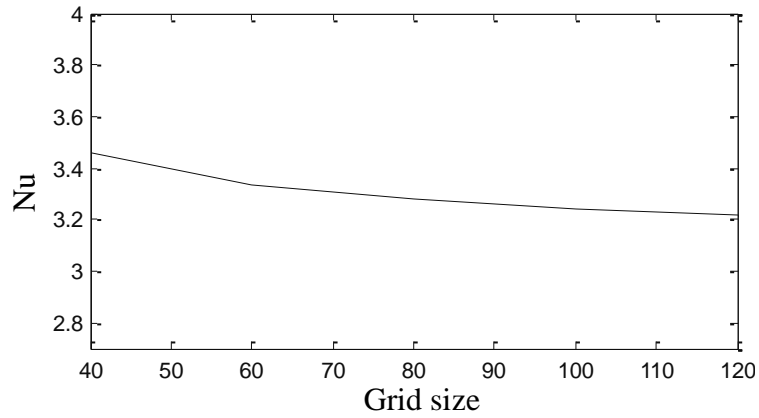
Fig. 2 Grid dependency curve. Ra=1000, Ø=0.1, D=0.1
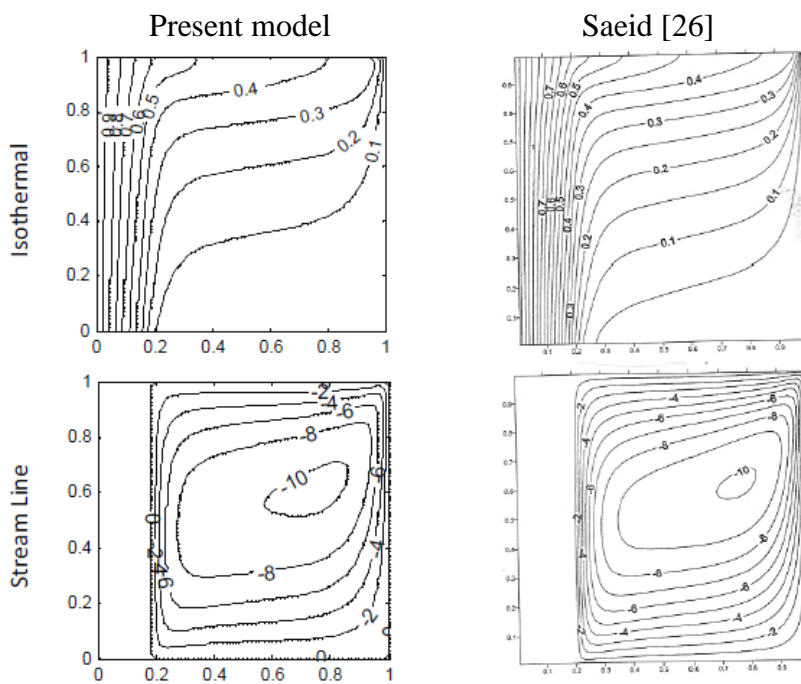
Fig. 3 Comparision with [38] streamlines and isotherms sample
$D = 0.2, Ø = 0.0, k_{wf} = 1, Ra=1000$
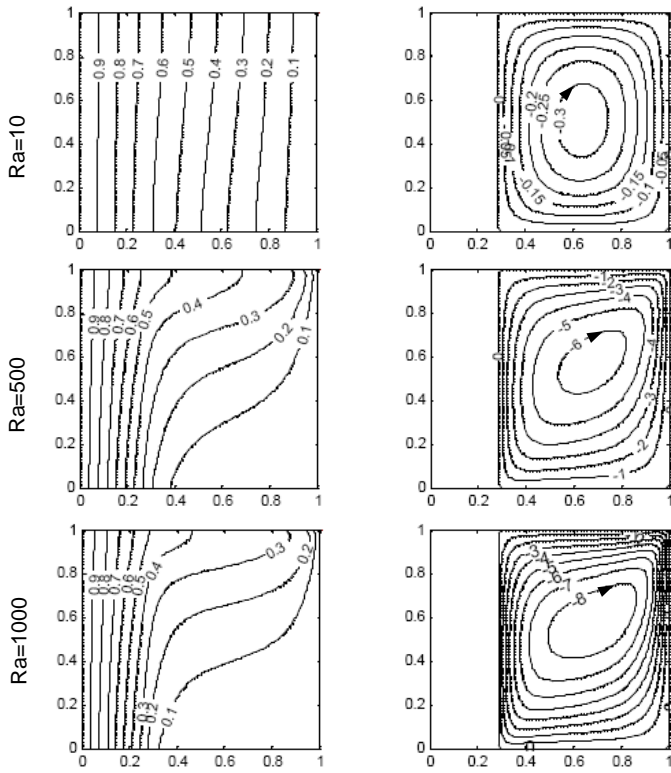
Fig.4 Isotherms (on the left) and Streamlines (on the right) and for Cu-water nanofluids D = 0.3, Ø = 0.1, k_wf = 1
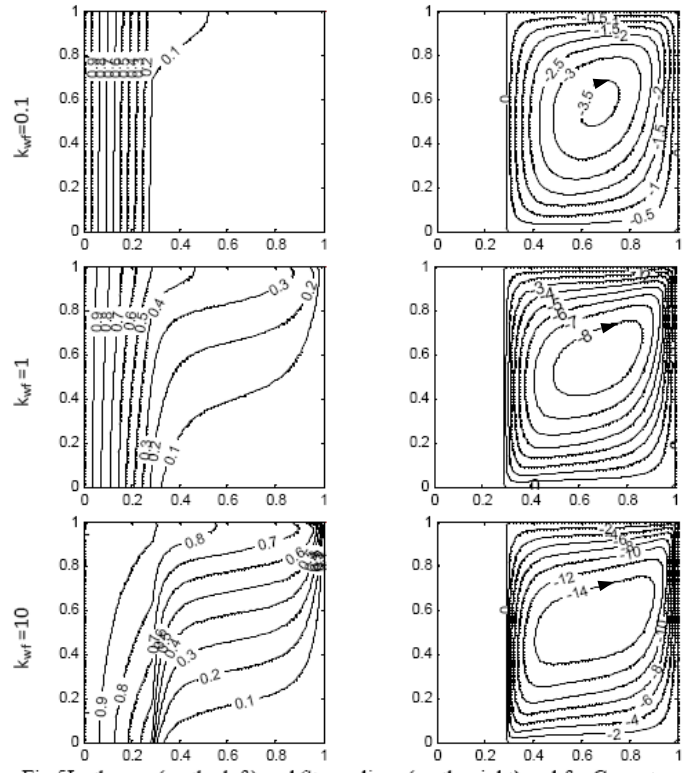
Fig.5 Isotherms (on the left) and Streamlines (on the right) and for Cu-water nanofluid D = 0.3, Ø = 0.1, Ra= 1000
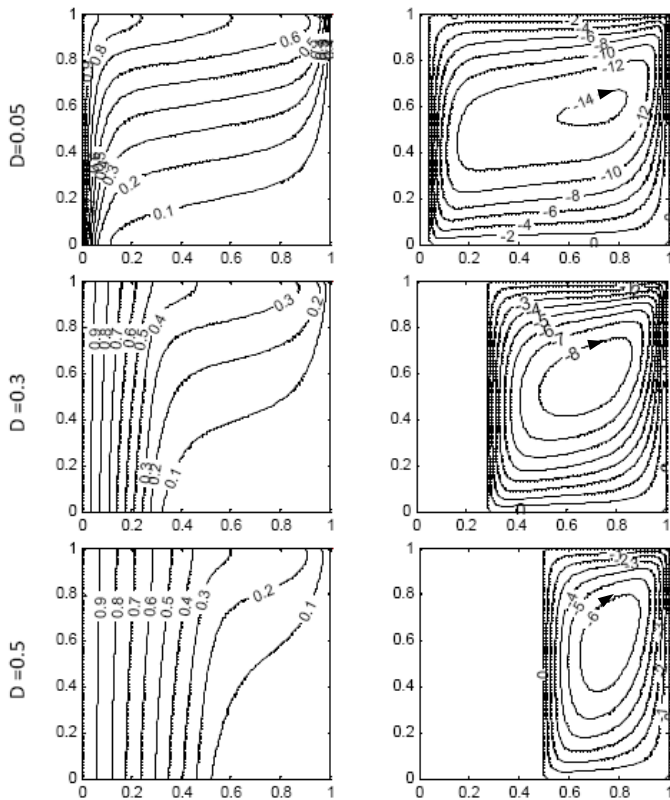
Fig.6 Isotherms (on the left) and Streamlines (on the right) and for Cu-water nanofluid k_wf = 1, Ø = 0.1, Ra= 1000
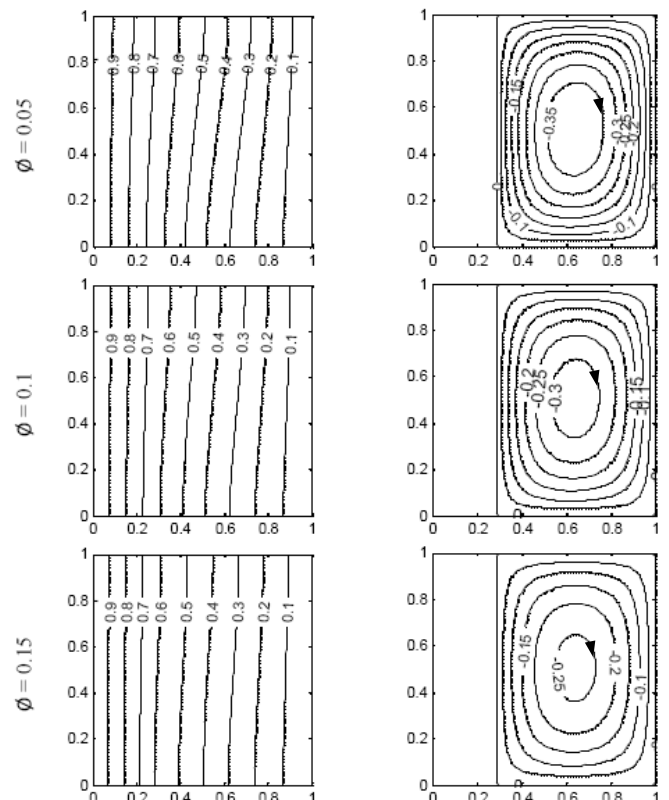
Fig.7 Isotherms (on the left) and Streamlines (on the right) and for Cu-water nanofluid k_wf = 1, D=0.3, Ra= 10
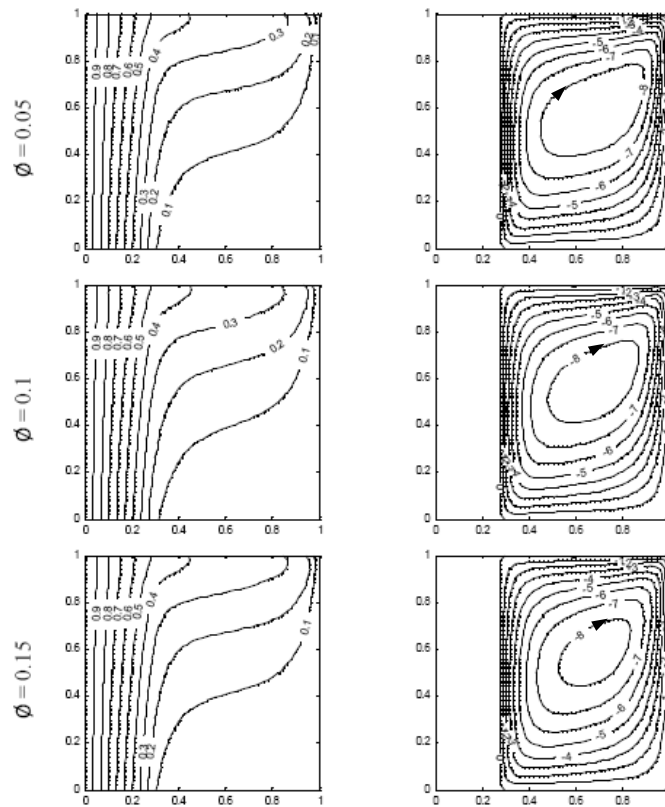
Fig.8 Isotherms (on the left) and Streamlines (on the right) and for Cu-water nanofluid $k_{wf} = 1$, D=0.3, Ra= 1000
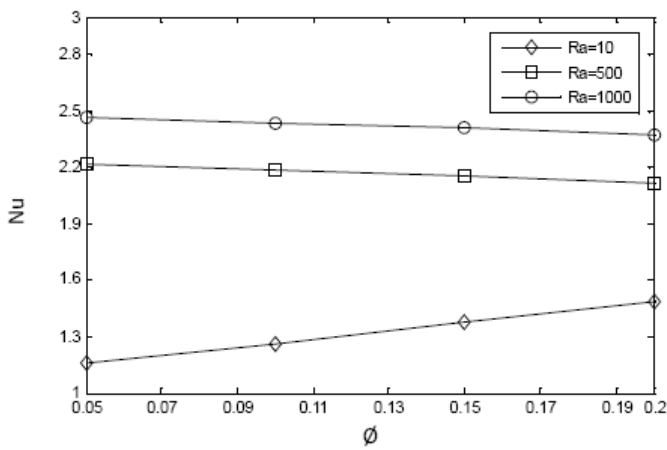
Fig.9 Dependence of the average Nusselt number on nanoparticle volume fraction (Ø) for different Rayleigh number (Ra) (D=0.3 , k_{wf}=1)
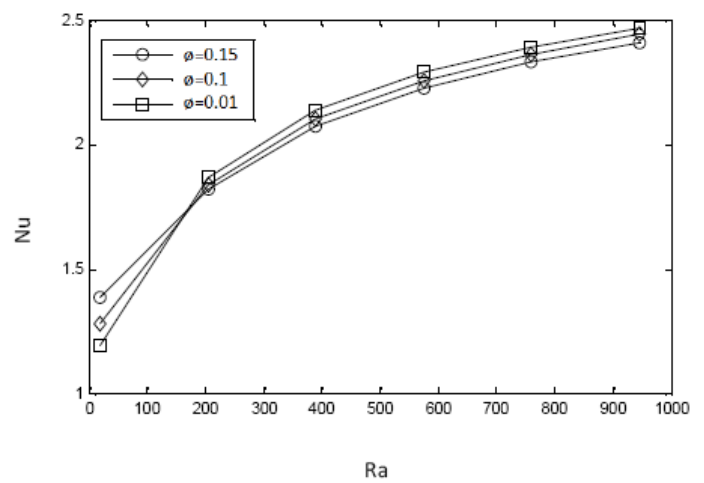
Fig.10 Dependence of the average Nusselt number on Rayleigh number for different nanoparticle volume fraction (Ø) (D=0.3 , k_{wf}=1)
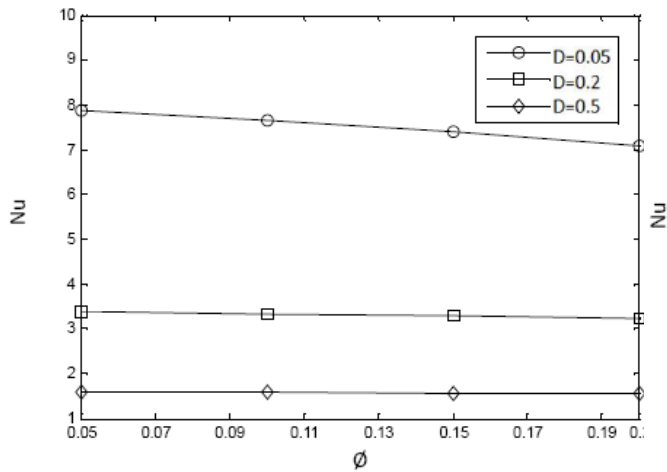
Fig.11 Dependence of the average Nusselt number on nanoparticle volume fraction (ø) for different thickness ratio of the wall (D) (k_{wf}=1 , Ra=1000)
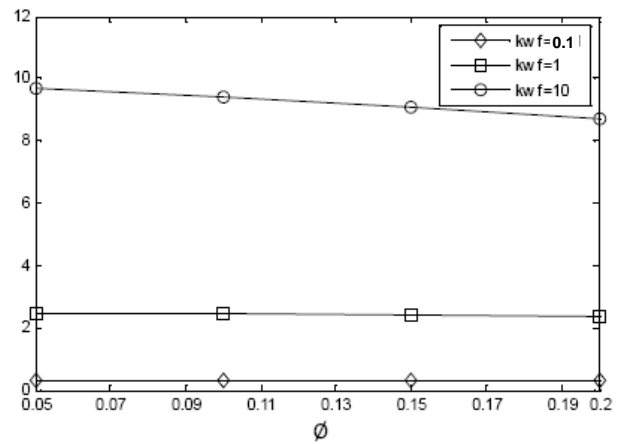
Fig.12 Dependence of the average Nusselt number on nanoparticle volume fraction (Ø) for different thermal conductivity ratio (k_{wf}) (D=0.3 , Ra=1000)
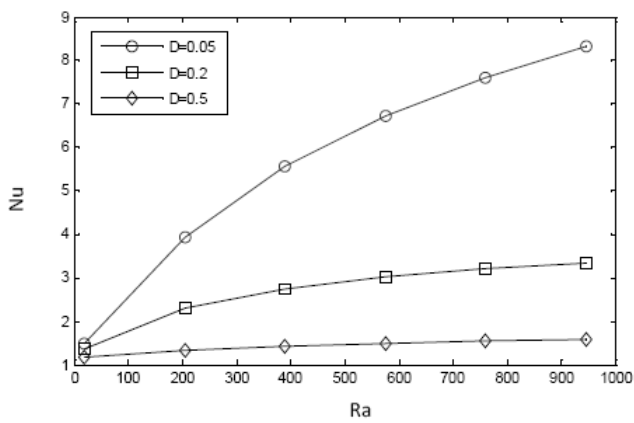
Fig.13 Dependence of the average Nusselt number on Rayleigh number for different thickness ratio of the wall (Ø =0.1 , k_{wf}=1)
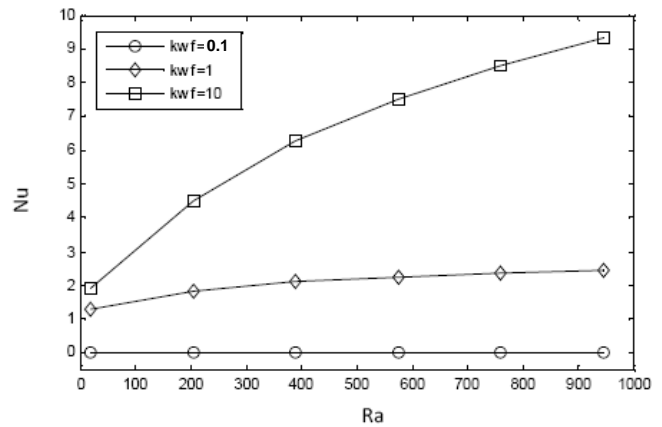
Fig.14 Dependence of the average Nusselt number on Rayleigh number for different thermal conductivity ratio (k_{wf}) (Ø =0.1 , D=0.3)
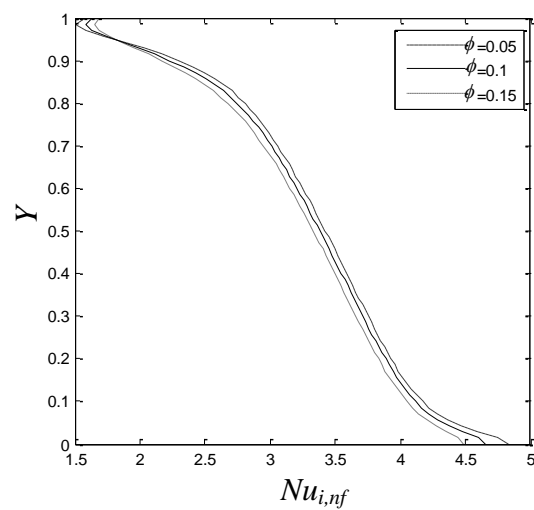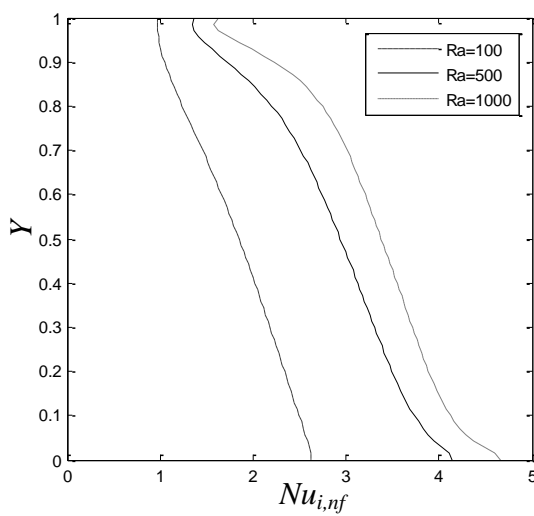
Fig. 15 Local Nusselt number along the interface Eq. (16), for D=0.2, k_{wf}=1.0, (a) ϕ =0.1, (b) Ra=1000

Appendix A: Finite differences formulas

Solid domain:

$$\theta_{i,j} = \frac{\theta_{i+1,j} + \theta_{i-1,j} + \theta_{i,j+1} + \theta_{i,j-1}}{4}$$

Porous domain:

$$\theta_{i,j} = \frac{1}{c}\left(\theta_1 + \theta_2 + \theta_3 + \theta_4\right)$$

where:

$$c = \frac{2Ar}{\Delta x^2} + \frac{2Ar}{\Delta y^2}$$

$$Ar = \frac{\alpha_{nf}}{\alpha_f}$$

$$\theta_1 = \theta_{i+1,j}\left[\left(\frac{\Psi_{i,j-1} - \Psi_{i,j+1}}{4\Delta x\Delta y}\right) + \frac{Ar}{\Delta x^2}\right]$$

$$\theta_2 = \theta_{i-1,j}\left[\left(\frac{\Psi_{i,j+1} - \Psi_{i,j-1}}{4\Delta x\Delta y}\right) + \frac{Ar}{\Delta x^2}\right]$$

$$\theta_3 = \theta_{i,j+1}\left[\left(\frac{\Psi_{i+1,j} - \Psi_{i-1,j}}{4\Delta x\Delta y}\right) + \frac{Ar}{\Delta y^2}\right]$$

$$\theta_4 = \theta_{i,j-1}\left[\left(\frac{\Psi_{i-1,j} - \Psi_{i+1,j}}{4\Delta x\Delta y}\right) + \frac{Ar}{\Delta y^2}\right]$$
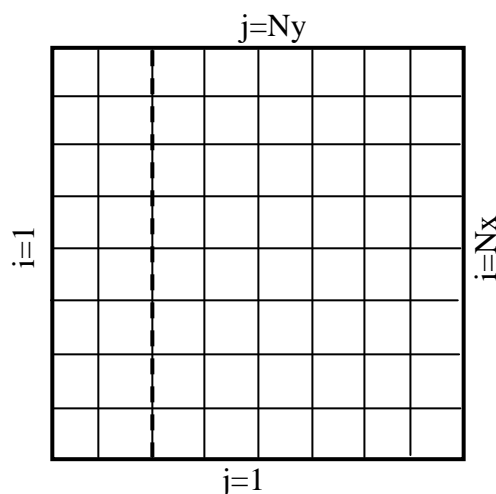
Top boundary nodes:
The same relations above but replacing the index j+1 with j-1 ($\frac{\partial\theta}{\partial y} = 0, \frac{\partial\Psi}{\partial y} = u = 0$)

Bottom boundary nodes:
The same relations above but replacing the index j-1 with j+1 ($\frac{\partial\theta}{\partial y} = 0, \frac{\partial\Psi}{\partial y} = u = 0$)

Corner nodes
The four corner nodes are included within the isothermal sides.

Appendix B: Steps of numerical calculations

(1) Set the values D , L , kw , Ra , ks , kf , α_f , N, Ø ,Cp_s , Cp_f , ρ_f , ρ_s

⬇

(2) Calculate k_r , k_{nf} , Cp_{nf} , α_{nf} , ρ_{nf}

⬇

(3) Set the initial values for θ_w , θ_{nf} , Ψ in each nods (N x N)

⬇

(4) Set the boundary conditions:
θ_w=1 at x=0, θ_{nf} =0 at x=1, $\partial\theta/\partial Y$=0 at Y=0 and at Y=1
Ψ=0 throughout solid boundaries.

⬇

(5) Calculate a new value of θ_w for each nodes which lie in the wall ($0<x<D$) from Eq.13 and then calculate the deference between the old and new value which will equal (error 1) in each nodes.
A_i, B_i, C_i, F_i

⬇

(6) Calculate a new value of θ_{nf} for each nods which lie in the nanofluid ($D<x<1$) from Eq.12 and then calculate the deference between the old and new value which will equal (error2) in each nods.

⬇

(7) Calculate a new value of Ψ for each nods which lie in the nanofluid (D<x<1) from Eq.11 and then calculate the deference between the old and new value which will equal (error3) in each nods.

⬇

(8) Find the maximum error from matrixes (error1, error2 & error3)

If maximum error ≤ 1E-05 — Yes

NO

(9) Set the new value instead the old for θ_w , θ_{nf} , Ψ

(9) End